Biol. Chem., Vol. 385, pp. 913–920, October 2004 • Copyright © by Walter de Gruyter • Berlin • New York. DOI 10.1515/BC.2004.119

Review

Inter- and intra-molecular distances determined by EPR spectroscopy and site-directed spin labeling reveal protein-protein and protein-oligonucleotide interaction

Heinz-Jürgen Steinhoff

Fachbereich Physik, Universität Osnabrück, D-49069 Osnabrück, Germany
e-mail: hsteinho@uos.de

Abstract

Recent developments including pulse and multi-frequency techniques make the combination of site-directed spin labeling and electron paramagnetic resonance (EPR) spectroscopy an attractive approach for the study of protein-protein or protein-oligonucleotide interaction. Analysis of the spin label side chain mobility, its solvent accessibility, the polarity of the spin label micro-environment and distances between spin label side chains allow the modeling of protein domains or protein-protein interaction sites and their conformational changes with a spatial resolution at the level of the backbone fold. Structural changes can be detected with millisecond time resolution. Inter- and intra-molecular distances are accessible in the range from approximately 0.5 to 8 nm by the combination of continuous wave and pulse EPR methods. Recent applications include the study of transmembrane substrate transport, membrane channel gating, gene regulation and signal transfer.

Keywords: bacteriorhodopsin; inter-spin distance; proline permease; pulse EPR; sensory rhodopsin.

Introduction

The understanding of protein, DNA or RNA function and interaction requires the knowledge of the respective molecular structures and their conformational dynamics. Crystallization of membrane proteins or protein complexes is still challenging and conformations found in the crystallized molecules may not represent the catalytically or biologically active ones (Perozo et al., 1999; Fanucci et al., 2003). Therefore, the development of complementary spectroscopic techniques, like fluorescence resonance energy transfer (FRET), solid state nuclear magnetic resonance (NMR), and electron paramagnetic resonance spectroscopy (EPR) is necessary for obtaining structural and dynamic information under physiological conditions.

During the last decade EPR spectroscopy in combination with site-directed spin labeling (SDSL) and molecular dynamics (MD) simulations has emerged as a powerful method for studying the structure and conformational dynamics of proteins and nucleic acids under conditions relevant to function (Hubbell et al., 1996, 1998, 2000; Feix and Klug, 1998; Steinhoff, 2002). Spin label side chains are introduced at selected sites via cysteine substitution mutagenesis followed by modification of the sulfhydryl groups with a specific paramagnetic nitroxide reagent (Berliner et al., 1982; Figure 1). Other accessible native cysteines have to be replaced before by e.g. serines or alanines. The continuous wave (cw) EPR spectrum yields information about the nitroxide side chain mobility (for a recent review see e.g. Columbus and Hubbell, 2002), its solvent accessibility (Hubbell and Altenbach, 1994), the polarity of its immediate environment or the distance between two nitroxides. Recently, the sensitivity toward polarity and polarity changes in the vicinity of the nitroxide side chain has been dramatically increased by the application of high-frequency, high-field (95 GHz, 3.4 T) EPR spectroscopy (Steinhoff et al., 2000b; Wegener et al., 2001b). EPR data analysis of a series of spin-labeled variants of a given protein allows the definition of secondary structure elements (including their solvent exposure), to characterize protein topography and to determine orientations of individual segments of the protein. A complete analysis thus leads to a model of the protein structure with a spatial resolution at the level of the backbone fold (Hubbell et al., 1998; Perozo et al., 1998; Koteiche and Mchaourab, 1999; Hubbell et al., 2000; Mchaourab and Perozo, 2000; Wegener et al., 2001a). In many cases sample volumes of less than 5 μl

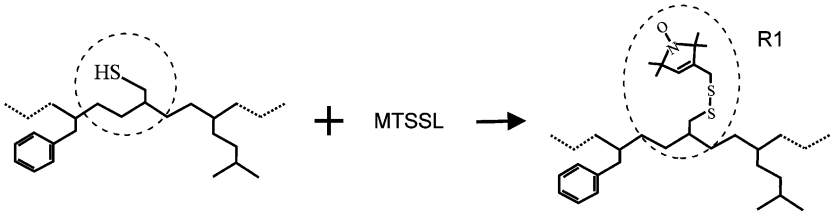

Figure 1 The reaction of the methanethio-sulfonate spin label (MTSSL) (Berliner et al., 1982) with a sulfhydryl group generates the spin label side chain R1.

and protein concentrations less than 50 μM are sufficient to obtain the desired information. The method is applicable to any protein or oligonucleotide that retains its function after spin labeling. One of the most powerful properties of the method is its sensitivity to molecular dynamics: protein equilibrium fluctuations and conformational changes of functional relevance can be followed on a wide time scale ranging from picoseconds to seconds.

This review focuses on recent developments of EPR-based inter-spin distance measurements of spin-labeled proteins and applications revealing mechanisms of protein-protein or protein-oligonucleotide interaction. The combination of cw and pulse EPR spectroscopy enables determination of inter- and intra-molecular distances in the range from 0.5 to 8 nm (Figure 2). The methods will be illustrated with a few model systems which are currently under investigation in our laboratory: the light-driven proton pump bacteriorhodopsin is a membrane protein of well-known structure (Essen et al., 1998; Luecke et al., 1999) which is often used for the development and improvement of novel methods. The sensory rhodopsin-transducer complex, pSRII-pHtrII, responsible for the negative phototaxis of archaea, may be regarded as a model system for signal transduction (Klare et al., 2004b). The Na^+/proline transporter PutP is an interesting model for the Na^+/substrate symporter family (SSSF) which currently comprises more than 200 similar proteins of pro- and eukaryotic origin (Jung, 2001). Finally, protein-oligonucleotide interaction is exemplified with tetracycline repressor (TetR)-DNA interaction and reverse transcriptase (RT)-DNA interaction.

Inter-spin distance measurements: methods and applications

Distance measurements by magnetic resonance methods are based on the distance dependence of the dipole-dipole coupling between two spins. In general, the magnetic interaction between two spin labels attached to a protein is composed of static dipolar interaction, modulation of the dipolar interaction by the residual motion of the spin label side chains and exchange interaction. The static dipolar interaction leads to considerable broadening or dipolar splitting of the cw EPR spectrum if the inter-spin distance is less than 2 nm. In order to prevent motional averaging of the dipolar interaction, samples have to be measured in solutions of high viscosity (Altenbach et al., 2001) or in the frozen state below 200 K (Steinhoff et al., 1991, 1997; Rabenstein and Shin, 1995). For unique orientations of the nitroxides relative to each other as found for spin labels introduced at buried sites, a rigorous solution of the spin Hamiltonian can be obtained. Spectra simulations and fittings to experimental EPR data determined at 9 GHz, 35 GHz and 95 GHz yield the distance between the nitroxides and the Euler angles describing their relative orientation and that of the inter-spin vector relative to the magnetic field (Hustedt et al., 1997; Hustedt and Beth, 1999). A detailed discussion of resolved splittings due to electron dipolar couplings has been published earlier (Eaton et al., 2000).

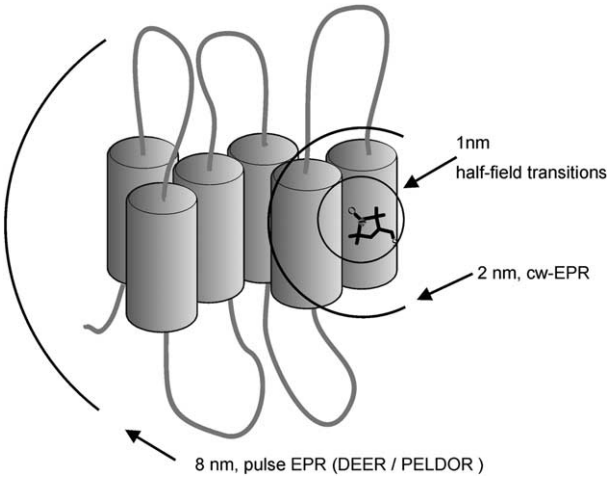

Figure 2 Applications of different EPR methods span the range of accessible inter-spin distances from about 0.5 nm to 8 nm. Relative amplitudes of forbidden half-field transitions and allowed transitions are sensitive in the distance range up to 1 nm (Eaton et al., 1983). Line shape analysis of cw EPR spectra allow reliable determination of distances in the range from about 0.8 to 2 nm (Rabenstein and Shin, 1995; Steinhoff et al., 1997). Beyond 2 nm the contribution of dipolar broadening to the spectral line width is negligible. Here pulse EPR or pulse ELDOR methods have to be applied which expand the accessible distance range up to 8 nm (Jeschke et al., 2004a).

For surface sites, the nitroxides usually adopt a statistical distribution of distances and relative orientations within a restricted distance and orientation range. Here, the following approximation yields acceptable results. According to an approach given by Ciecierska-Tworek et al. (1973) the absorption lines of a pair of interacting spins are shifted from the resonance positions without dipolar interaction by

$$\Delta B = \pm \frac{3g\beta_e(3\cos^2\theta - 1)}{4\rho^3},$$

where θ is the angle between the magnetic field B_0 and the distance vector ρ between the two interacting spins, β_e denotes the Bohr magneton and g is an average g value of the nitroxides. In a frozen solution or powder sample we expect an isotropic orientation distribution of the distance vectors between the interacting spins. The corresponding dipolar spectrum of such a macroscopically disordered sample calculated from the above equation is a Pake pattern. The range of inter-spin distances arising from a distribution of protein conformations or orientations of the spin label side chains is accounted for by a proper distribution function. In many cases a Gaussian distribution has been found to represent a reasonable approximation (see Figure 3B, inset) (Steinhoff et al., 1997). The final dipolar broadened EPR spectrum is calculated from the nitroxide powder spectrum by convolution with the Pake pattern. Values of inter-spin distances are finally determined by fitting of the calculated EPR spectra to the experimental spectra (Steinhoff et al., 1991, 1997; Radzwill et al., 2001). Alternatively, the dipolar broadened experimental spectrum of the doubly spin-labeled protein may be deconvoluted with the superposition spectra of the corresponding singly labeled

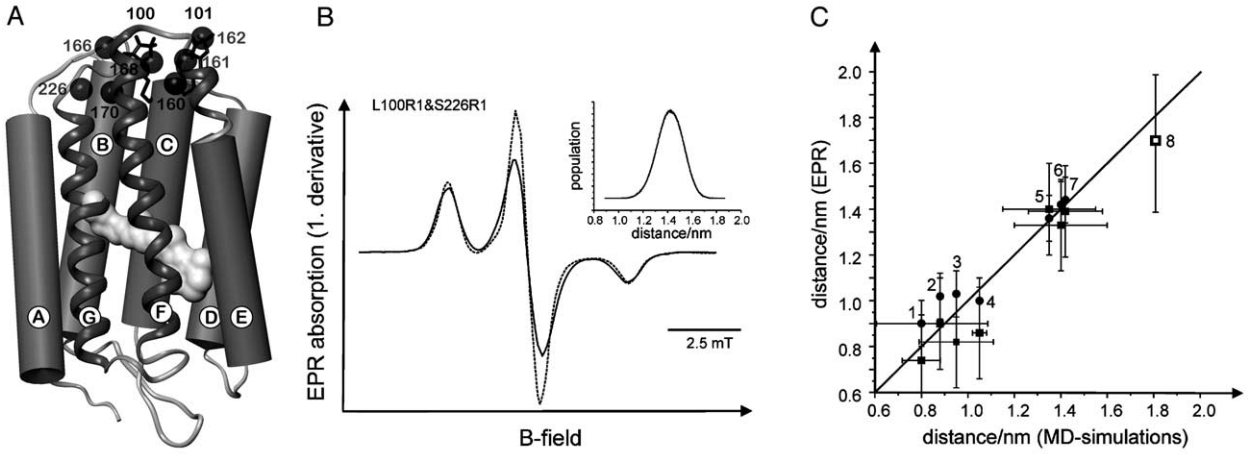

Figure 3 Distances between spin-labeled sites of bacteriorhodopsin.
(A) X-ray structure of the light-driven proton pump bacteriorhodopsin (Essen et al., 1998). Residues which were exchanged by cysteines and modified with the nitroxide spin label MTSSL are shown as spheres, spin label side chains are shown for positions 100 and 101. (B) Examples of experimental cw EPR spectra (T=170 K) of the bacteriorhodopsin double mutant 100R1&226R1 (continuous line) and the superposition of the spectra of the respective single mutants (broken line). The EPR spectrum of the doubly spin-labeled bacteriorhodopsin mutant is significantly broadened by dipolar interaction. Fitting of a simulated powder spectrum with DIPFIT (Radzwill et al., 2001) to the experimental spectrum yields an inter-spin distance of 1.4 nm with a distribution width of 0.2 nm. The inset shows the inter-nitroxide distance distribution of that sample determined from a 6 ns MD simulation trajectory with the backbone atoms restraint according to the X-ray structure (Steinhoff et al., 2000a). (C) Comparison of distances determined for nitroxide pairs bound to different sites in bacteriorhodopsin (Radzwill, 2001; Radzwill et al., 2001; closed symbols) or hexameric insulin (Steinhoff et al., 1997; open symbol) with values calculated from MD simulations. Fitting of simulated cw EPR powder spectra provide mean distances (squares) and distance distribution widths (error bars). Alternatively, distance values were estimated from the second spectral moment (circles). The error bars of the values determined by MD simulations reflect the distance distribution widths as determined from trajectories of 6 ns length (Steinhoff et al., 2000a) [1, 101–168; 2, 101–160 (the mean of two appearing distance population maxima at 0.6 and 1.1 nm is depicted); 3, 101–161; 4, 101–170; 5, 101–166; 6, 101–226; 7, 100–226; 8, B2 nitroxide position of spin-labeled crystallized insulin R6].

proteins. The inter-spin distance is extracted from the shape of the resulting Pake pattern (Rabenstein and Shin, 1995). The lower limit for reliable distance determination using the above methods is given by the increasing influence of exchange interaction for inter-spin distances of less than 0.8 nm due to partial overlap of the nitrogen π-orbitals of the two interacting nitroxides. In this distance regime, half field transitions, which are not sensitive to exchange interaction, have been successfully applied (Eaton et al., 1983; Steinhoff et al., 1997; Persson et al., 2001). A detailed discussion of the influence of exchange coupling on the above approximations can be found in a recent review (Jeschke, 2002a). Since the spin labeling efficiency may be less than 100% a variable fraction of singly spin-labeled protein has to be accounted for in the above approaches. The spectra simulation and deconvolution methods for inter-spin distance determination have been successfully validated by comparison of EPR data with crystallographic data of spin-labeled insulin (Steinhoff et al., 1997), lysozyme (Altenbach et al., 2001), bacteriorhodopsin (Radzwill et al., 2001) or with synthesized spin-labeled peptides of known secondary structure (Rabenstein and Shin, 1995). Figure 3 shows a comparison of distances between different spin-labeled sites of bacteriorhodopsin determined by cw EPR (T=170 K) with average distance values calculated from MD simulations. During these simulations the backbone of bacteriorhodopsin was restrained according to X-ray crystallographic data (Essen et al., 1998) and only the side chains including the nitroxide side chains R1 were free to move. MD simulations at high temperature (400 to 600 K) were performed to allow the nitroxides to cover the accessible space within trajectory lengths of 6 ns (Steinhoff et al., 2000a). The results confirmed that the convolution of powder spectra with the Pake pattern is a valid approximation if the spin label side chains are frozen in different orientations.

The line width of the spectra is a steep function of the inter-spin distance. Hence, empirical or semi-empirical parameters as spectral amplitude ratios or spectral second moment values are often sufficient to answer structural questions (Mchaourab and Perozo, 2000; Radzwill et al., 2001). In particular, a simplified inter-spin distance estimation using the difference of spectral second moments is not influenced by exchange interaction and less sensitive to spectral contributions of singly labeled proteins (Radzwill et al., 2001; Steinhoff, 2002) than the convolution/deconvolution techniques. Distance values determined from the spectral second moment of doubly spin-labeled bacteriorhodopsin agree with the values determined from spectral fitting (see Figure 3). Besides nitroxide-nitroxide interaction also metal ion-nitroxide interactions in metalloproteins or engineered copper ion-binding sites allow estimation of intra-molecular distances (Leigh, 1970; Voss et al., 1995a,b).

For inter-spin distances exceeding 2 nm the line broadening due to dipolar interaction is much less than the influence of other homogeneous and inhomogeneous contributions, hence cw EPR is not sensitive for dipolar interactions. However, the application of pulse double resonance EPR methods increases the accessible distance range up to 8 nm. These techniques include four-pulse double electron-electron resonance (DEER)

(Pannier et al., 2000; Jeschke, 2002b), the 2+1 pulse sequence (Kurshev et al., 1989), multiple-quantum EPR (Borbat and Freed, 1999), and single-frequency techniques for refocusing (SIFTER) electron-electron couplings (Jung et al., 1995; Jeschke et al., 2000). Recently, a pulse EPR spectroscopic ruler for oligonucleotides was developed using a series of spin-labeled duplex DNAs (Schiemann et al., 2004). Recent developments lead to considerable enhancement of the sensitivity of the pulse DEER technique which allows investigations of membrane proteins in their native environment (Jeschke et al., 2004a,b).

Since the first quantitative analysis of dipolar splitting observed in a spin-labeled protein (Deparade et al., 1981) the method of inter-spin distance determination by cw EPR spectroscopy has been successfully applied to reveal domain structures of membrane proteins, including rhodopsin (Altenbach et al., 1996; Cai et al., 1997), lac permease (Voss et al., 1998) and the KcsA potassium channel (Perozo et al., 1998, 1999). In addition, changes in dipolar interaction result in large spectral changes, making it straightforward to monitor conformational changes (Farrens et al., 1996; Perozo et al., 1999; Tiebel et al., 1999). Recent notable successes include the evaluation of the gating mechanism of the mechanosensitive channel MscL (Perozo et al., 2002; Perozo and Rees, 2003). Changes of the protein secondary structure, protein tertiary fold or domain movements can be followed with up to 0.1 ms resolution with conventional cw EPR instrumentation and detection schemes. Interesting examples are the detection of rigid body helix motion in both rhodopsin and bacteriorhodopsin (Farahbakhsh et al., 1993; Steinhoff et al., 1994; Farrens et al., 1996; Thorgeirsson et al., 1997; Xiao et al., 2000; Radzwill et al., 2001), domain movements in T4 lysozyme (Hubbell et al., 1996), and conformational changes during signal transfer from sensory rhodopsin pSRII to the transducer pHtrII (Wegener et al., 2001a). Examples are discussed in detail in the following paragraphs.

Inter-spin distance determination by four-pulse DEER: proline permease (PutP)

PutP is a member of the Na^+/substrate symporter family (SSSF) which currently comprises more than 200 similar proteins of pro- and eukaryotic origin (Jung, 2001). These integral membrane proteins utilize the Na^+ electrochemical gradient to drive the transport of a variety of substrates like sugars, amino acids and vitamins. Biochemical and biophysical studies including EPR spectroscopy suggest a secondary structure model according to which PutP contains 13 transmembrane helices (TMs) with the N-terminus located on the periplasmic side of the membrane and the C-terminus facing the cytoplasm (Jung et al., 1998; Wegener et al., 2000b; Figure 4). PutP is thought to undergo a series of conformational transitions such that the ligand-binding sites are alternatively accessible to one side of the membrane or the other. EPR spectroscopy data of singly spin labeled PutP variants (Wegener et al., 2000b) in the presence and absence of Na^+ or proline revealed that binding of ligands induces conformational alterations that involve at least part of TM II and the preceding cytoplasmic loop (loop L2). With doubly spin-labeled variants L37C&A107C and L37C&D187C distances were determined between the cytoplasmic loops L2 and L4 and between the loops L2 and L6. In addition, the PutP derivative A107C&S223C provide nitroxides positions which were assumed to be located on different sides of the lipid membrane (loops L4 and L7).

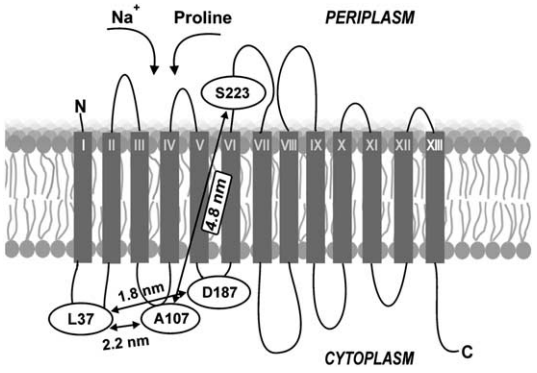

Figure 4 Secondary structure model of PutP with the spin-labeled sites highlighted.
Given are the mean distances between these sites as determined by four-pulse DEER (Jeschke et al., 2004b). The observed increase of the distance between loops L2 and L6 upon Na^+ binding reveals substrate-triggered conformational changes of the protein.

Cw EPR spectroscopy revealed that the average intramolecular distances in all samples exceeded 1.8 nm, which is close to the upper limit of the convolution or deconvolution method for reliable distance determination. Hence we applied a model-free direct transformation of four pulse DEER time domain data with the crosstalk-corrected approximate Pake transformation (Jeschke et al., 2002). For L37C&D187C the maximum of the distance distribution was found to be close to the lower distance limit of the pulse DEER method (~1.8 nm) and the asymmetric width of the distribution was estimated to approach 0.8 nm. The results suggest that the loops L2 and L6 are in close proximity and that these regions are very flexible. R40 in the vicinity of L37 plays an important role in coupling of Na^+ and proline transport (Quick et al., 1999). Similarly, D187 in loop L6 is crucial for an efficient coupling of the transport of both ligands (Quick and Jung, 1998). Both residues are highly conserved within the SSSF. The functional importance of these sites is even more pronounced by the observation that the distance between positions 37 and 187 increased upon Na^+ binding. The large value of 4.8 nm for the inter-spin distance determined between position 107 in loop 4 and position 223 in loop 7 is in agreement with the assumption that these positions are located on opposite sides of the membrane. The above results demonstrate that the sensitivity of four-pulse DEER spectroscopy allows investigation of the structure and conformational changes of integral membrane proteins reconstituted in liposomes with sample volumes of less than 50 μl.

Protein-nucleic acid interaction: Tet repressor and reverse transcriptase interacting with DNA

Many proteins active in the regulation of transcription are triggered by effectors to switch between DNA-binding and non-binding states. The crystal structures of the inducer-free TetR and the TetR-($[Mg\text{-}tc]^+$)$_2$-complex (Hinrichs et al., 1994; Kisker et al., 1995), and the characterization of non-inducible TetR mutants (Hecht et al., 1993; Müller et al., 1995) have suggested conformational changes of the protein upon tetracycline (tc) binding. High intrinsic flexibility is also required for the function of the human immunodeficiency virus type 1 (HIV-1) reverse transcriptase (RT), which has to bind successively the primer/templates tRNA/RNA, DNA/RNA, RNA/DNA and DNA/DNA during the conversion of single-stranded viral RNA into double stranded DNA (Skalka and Goff, 1993). Inter-spin distance measurements uncovered details of the conformational changes of TetR and RT upon interaction with nucleic acid substrates or inhibitors in solution (Tiebel et al., 1999; Kensch et al., 2000a,b) (for a recent review see Steinhoff and Suess, 2003). Nitroxide side chains introduced at sites I22R1/I22R1′ and N47R1/N47R1 in the DNA reading heads and different positions in the core of TetR (a prime notes residues from the second monomer) reveal at least two different conformations in the tc- or DNA-bound and free proteins in frozen and liquid solution. The binding of tc results in a decrease of the distances between positions 22 and 22′ in the order of 0.5 nm and an increase of the distance between positions 47 and 47′ of similar extent. This reflects a twisting motion of the DNA reading heads with respect to each other that modulates binding to two adjacent major grooves of B-form DNA (Tiebel et al., 1999; Orth et al., 2000).

X-ray structures of unliganded HIV-1 RT, RT bound to different inhibitors and to a DNA/DNA p/t (for a review see Jager and Pata, 1999) reveal the most prominent difference among these structures to occur for the p66 thumb subdomain, which undergoes a 30°–40° rigid-body movement relative to the p66 palm subdomain on going from the unliganded enzyme to the nucleic acid substrate bound form. This results in an opening of the structure (open conformation), generating a large nucleic acid binding cleft. It has been proposed that the underlying flexibility may play an essential role in the polymerization process, enabling the growing nucleic acid chain to translocate along the enzyme after each nucleotide incorporation step. The conformations of different RT complexes in solution under conditions relevant to function were characterized in terms of the distances between nitroxides bound to the fingers and thumb domains at positions 24 (fingers) and 287 (thumb) of p66 (Kensch et al., 2000a,b). These EPR measurements revealed a temperature-dependent equilibrium between the closed and open conformation of unliganded RT with the fraction of the open conformation varying between 35% at 272 K and 5% at 313 K (Kensch et al., 2000b). The presented results demonstrate that the p66 thumb domain of HIV-1 RT is highly flexible in solution, adopting two defined conformations. This is in perfect agreement with the available X-ray structures of the enzyme and confirms that the observed structures are not a result of crystal packing artifacts.

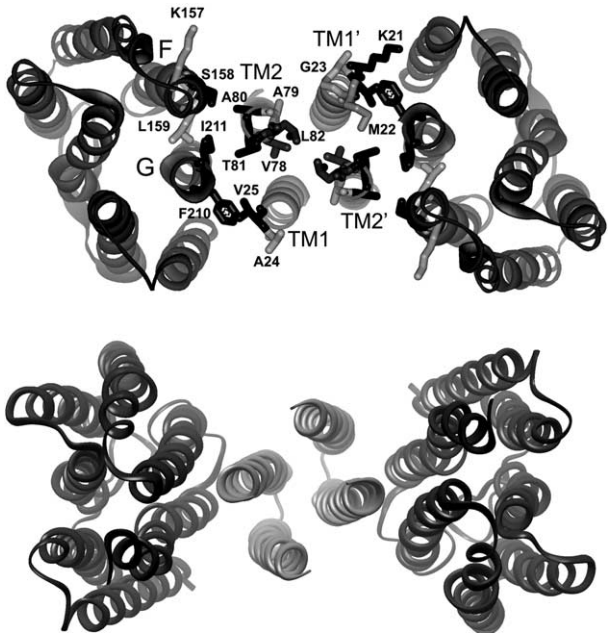

Figure 5 Transmembrane portion of the 2:2-complex of pSRII with its transducer pHtrII (view from the cytoplasm).
Inter-spin distances determined for 26 combinations of site-directed spin-labeled (marked positions) pSRII and pHtrII enabled modeling of the location and relative orientations of the transmembrane helices of the transducer, TM1 and TM2, and of helices F and G of the receptor (Wegener et al., 2001a). Since structural data for pSRII were not available in 2001, bacteriorhodopsin was used as a template to orient the remaining helices. The overall topology of the complex agrees with the crystal structure (bottom) (Gordeliy et al., 2002).

Protein-protein interaction: the sensory rhodopsin-transducer complex

The archaeabacterial photoreceptor sensory rhodopsin II (SRII) provides the signal which enables the bacteria to seek favorable light conditions (for reviews, see Spudich, 1998; Spudich et al., 2000). The photoreceptor is tightly complexed to a receptor-specific transducer (HtrII) consisting of two transmembrane helices. The light-induced signal is transferred from the receptor to the cytoplasmic domain of the transducer which activates a two-component signaling cascade well known from bacterial chemotaxis. A structural model of the pSRII-pHtrII complex from *Natronobacterium pharaonis* was determined from an EPR-based distance analysis of a set of doubly spin-labeled protein variants reconstituted into purple membrane lipid bilayers (Wegener et al., 2001a). Inter- and intra-molecular spin-spin distances were obtained for 26 pairs of spin labels introduced into the transmembrane helices TM1 or TM2 of the transducer pHtrII and helices F or G of the receptor pSRII (Figure 5). Considerable spin-spin interactions observed for the singly labeled transducer with the nitroxide side chain located at positions 78 or 82 confirmed a dimeric arrangement

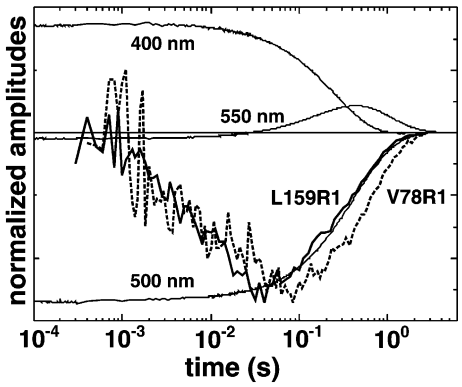

Figure 6 Optical absorption changes and EPR transients (noisy lines) of the receptor-transducer complex pSRII-pHtrV78R1 (broken line), and of L159R1-pHtrII (solid line) after light activation (T=293 K) (Klare et al., 2004b).
The transient increase of the mobility of the spin label side chain L159R1 indicates an outward movement of helix F of pSRII (Wegener et al., 2001a) similar to that found in BR (Radzwill et al., 2001). This leads to a conformational change of the transducer as revealed by the transient increase of the distance between positions 78 and 78′ in TM2 and TM2′.

of TM2 and TM2′. The closest distances (less than 1.2 nm) between pSRII and pHtrII were observed between the nitroxides of spin-labeled residues of both helices TM1 and TM2 and the receptor helix G. The 26 inter-spin distance values provided constraints for modeling of the pSRII-pHtrII structure with the assumption of parallel transmembrane helix orientations and the structure of pSRII resembling that of bacteriorhodopsin (Wegener et al., 2001a). The resulting quaternary complex of two molecules of pHtrII and pSRII each forms a structure with an apparent two-fold symmetry. The latter determined crystal structure of the complex was found to agree with the EPR derived model concerning the general topology, the location and relative orientation of the spin-labeled helices (Figure 5; Gordeliy et al., 2002; for a recent review comparing EPR and X-ray results cf. Klare et al., 2004a).

Upon light excitation the pSRII receptor reverts to the long-lived M-intermediate which was proposed to represent the signaling state (Yan et al., 1991). During this reaction helix F of the receptor moves outward similar to the conformational change found in BR (Wegener et al., 2000a; Radzwill et al., 2001). This helix movement of the receptor is transferred to the transducer as revealed by comparing the inter-residual distance changes observed between transducer/transducer as well as receptor/transducer (Wegener et al., 2001a; Klare et al., 2004b). Low temperature experiments (T=170 K) with the receptor trapped in the M intermediate showed decreases and increases of the interaction strengths between the TM2 and TM2′ and between TM2 and helix F of pSRII, respectively. The observed pattern of distance changes is in agreement with a transient clockwise rotation of TM2. In Figure 6 the time course of the EPR signal change of V78R1 at fixed magnetic field position is compared to that of L159R1. The nitroxides at positions V78R1 of TM2 and V78R1′ of TM2′ face each other leading to considerable dipolar broadening of the spectra. L159R1 is located in helix F and oriented toward the inside of the receptor. The optical absorptions monitoring the depletion and reformation of the pSRII ground state (500 nm) and of intermediates O (550 nm) and M (400 nm) are also depicted in Figure 6. The kinetic EPR difference spectra recorded at room temperature uncover a transient increase of the inter-spin distance for sample V78R1 and a transient mobilization for L159R1 (Wegener et al., 2001a). Thus, the signals shown in Figure 6 record events occurring at the level of the retinal chromophore, of helix F (L159R1, EPR trace), and of TM2 (V78R1, EPR trace) which allows to follow the signal transfer in the sequence retinal → helix F → TM2 and *vice versa*. After absorption of a photon by the retinal a synchronous conformational change of the sensor and the transducer is observed with a rise time of about 3 ms. This activated state remains unchanged for about 100 ms. With the reformation of the ground state, the reaction of the receptor seems to be decoupled from that of the transducer. The movement of helix F into the original position seems to precede the recovery of the TM2 position. This decoupling allows the system to modulate the activation/deactivation of the transducer, thereby enabling the bacteria to respond to external stimuli adequately (Wegener et al., 2001a).

Conclusion

The combination of site-directed spin labeling with cw and pulse EPR spectroscopy and MD simulations provide time-resolved information on conformational changes in protein-protein and protein-oligonucleotide complexes. This method allows elucidation of functional mechanisms involving conformational changes on the nanoscopic or mesoscopic scale like signaling, gating or gene regulation. Due to its high time resolution, its high sensitivity and the accessible distance range EPR spectroscopy ideally supplements other techniques like solid state NMR or FRET. New methods of spin labeling using artificial amino acids with nitroxide side chains and the application of multi-frequency EPR spectroscopy with magnetic fields ranging from 0.1 to 13 T will further enhance its potential.

Acknowledgments

The support by the Deutsche Forschungsgemeinschaft in the frames of the Schwerpunktprogramm SPP1051 and Sonderforschungsbereich SFB 431 is gratefully acknowledged.

References

Altenbach, C., Oh, K. J., Trabanino, R. J., Hideg, K. and Hubbell, W. L. (2001). Estimation of inter-residue distances in spin labeled proteins at physiological temperatures: experimental strategies and practical limitations. Biochemistry *40*, 15471–15482.

Altenbach, C., Yang, K., Farrens,D. L., Farahbakhsh, Z. T., Khorana, H. G. and Hubbell, W. L. (1996). Structural features and light-dependent changes in the cytoplasmic interhelical E-F loop region of rhodopsin – a site-directed spin-labeling study. Biochemistry *35*, 12470–12478.

Berliner, L. J., Grunwald, J., Hankovszky, H. O. and Hideg, K. (1982). A novel reversible thiol-specific spin label: papain active site labeling and inhibition. Anal. Biochem. *119*, 450–455.

Borbat, P. P. and Freed, J. H. (1999). Multi-quantum ESR and distance measurements. Chem. Phys. Lett. *313*, 145–154.

Cai, K. W., Langen, R., Hubbell, W. L. and Khorana, H. G. (1997). Structure and function in rhodopsin – topology of the C-terminal polypeptide chain in relation to the cytoplasmic loops. Proc. Natl. Acad. Sci. USA *94*, 14267–14272.

Ciecierska-Tworek, Z., Van, S. P. and Griffith, O. H. (1973). Electron-electron dipolar splitting anisotropie of a dinitroxide oriented in a crystalline matrix. J. Mol. Struct. *16*, 139–148.

Columbus, L. and Hubbell, W. L. (2002). A new spin on protein dynamics. Trends Biochem. Sci. *27*, 288–295.

Deparade, M. P., Gloggler, K. and Trommer, W. E. (1981). Isolation and properties of glyceraldehyde-3-phosphate dehydrogenase from a sturgeon from the Caspian Sea and its interaction with spin-labeled NAD^+ derivatives. Biochim. Biophys. Acta *659*, 422–433.

Eaton, G. R., Eaton, S. S. and Berliner, L. J. (2000). Distance Measurements in Biological Systems (New York, USA: Kluwer).

Eaton, S. S., More, K. M., Sawant, B. M. and Eaton, G. R. (1983). Use of the EPR half-field transition to determine the interspin distance and the orientation of the interspin vector in systems with two unpaired electrons. J. Am. Chem. Soc. *105*, 6560–6567.

Essen, L. O., Siegert, R., Lehmannn, W. D. and Oesterhelt, D. (1998). Lipid patches in membrane protein oligomers – crystal structure of the bacteriorhodopsin-lipid complex. Proc. Natl. Acad. Sci. USA *95*, 11673–11678.

Fanucci, G. E., Lee, J. Y. and Cafiso, D. S. (2003). Spectroscopic evidence that osmolytes used in crystallization buffers inhibit a conformation change in a membrane protein. Biochemistry *42*, 13106–13112.

Farahbakhsh, Z., Hideg, K. and Hubbell, W. L. (1993). Photoactivated conformational changes in rhodopsin: a time resolved spin label study. Science *262*, 1416–1420.

Farrens, D. L., Altenbach, C., Yang, K., Hubbell, W. L. and Khorana, H. G. (1996). Requirement of rigid-body motion of transmembrane helices for light activation of rhodopsin. Science *274*, 768–770.

Feix, J. B. and Klug, C. S. (1998). Site-directed spin labeling of membrane proteins and peptide-membrane interactions. In: Spin Labeling: The Next Millenium, L. J. Berliner, ed. (New York, USA: Plenum Press), pp. 251–281.

Gordeliy, V. I., Labahn, J., Moukhametzianov, R., Efremov, R., Granzin, J., Schlesinger, R., Büldt, G., Savopol, T. A., Scheidig, J. et al. (2002). Molecular basis of transmembrane signalling by sensory rhodopsin II-transducer complex. Nature *419*, 484–487.

Hecht, B., Müller, G. and Hillen, W. (1993). Noninducible Tet repressor mutations map from the operator binding motif to the C-terminus. J. Bacteriol. *175*, 1206–1210.

Hinrichs, W., Kisker, C., Düvel, M., Müller, A., Tovar, K., Hillen, W. and Saenger, W. (1994). Structure of the Tet repressor-tetracycline complex and regulation of antibiotic resistance. Science *264*, 418–420.

Hubbell, W. L. and Altenbach, C. (1994). Investigation of structure and dynamics in membrane proteins using site-directed spin labeling. Curr. Opin. Struct. Biol. *4*, 566–573.

Hubbell, W. L., McHaourab, H. S., Altenbach, C. and Lietzow, M. A. (1996). Watching proteins move using site-directed spin labeling. Structure *4*, 779–783.

Hubbell, W. L., Gross, A., Langen, R. and Lietzow, M. A. (1998). Recent advances in site-directed spin labeling of proteins. Curr. Opin. Struct. Biol. *8*, 649–656.

Hubbell, W. L., Cafiso, D. S. and Altenbach, C. (2000). Identifying conformational changes with site-directed spin labeling. Nat. Struct. Biol. *7*, 735–739.

Hustedt, E. J. and Beth, A. H. (1999). Nitroxide spin-spin interactions: applications to protein structure and dynamics. Annu. Rev. Biophys. Biomol. Struct. *28*, 129–153.

Hustedt, E. J., Smirnov, A. I., Laub, C. F., Cobb, C. E. and Beth, A. H. (1997). Molecular distances from dipolar coupled spin-labels – the global analysis of multifrequency continuous wave electron paramagnetic resonance data. Biophys. J. *72*, 1861–1877.

Jager, J. and Pata, J. (1999). Getting a grip: polymerases and their substrate complexes. Curr. Opin. Struct. Biol. *9*, 21–28.

Jeschke, G. (2002a). Determination of the nanostructure of polymer materials by electron paramagnetic resonance spectroscopy. Macromol. Rapid Commun. *23*, 227–246.

Jeschke, G. (2002b). Distance measurements in the nanometer range by pulse EPR. Chem. Phys. Chem. *3*, 927–932.

Jeschke, G., Pannier, M., Godt, A. and Spiess, H. W. (2000). Dipolar spectroscopy and spin alignment in electron paramagnetic resonance. Chem. Phys. Lett. *331*, 234–252.

Jeschke, G., Koch, A., Jonas, U. and Godt, A. (2002). Direct conversion of EPR dipolar time evolution data to distance distributions. J. Magn. Reson. *155*, 72–82.

Jeschke, G., Bender, A., Paulsen, H., Zimmermann, H. and Godt, A. (2004a). Sensitivity enhancement in pulse EPR distance measurements. J. Magn. Reson. *169*, 1–12.

Jeschke, G., Wegener, C., Nietschke, M., Jung, H. and Steinhoff, H.-J. (2004b). Inter-residual distance determination by four-pulse DEER in an integral membrane protein: the Na^+/proline transporter PutP of *Escherichia coli*. Biophys. J. *86*, 2551–2557.

Jung, H. (2001). Towards the molecular mechanism of Na^+/solute symport in prokaryotes. Biochim. Biophys. Acta *1505*, 131–143.

Jung, H., Rübenhagen, R., Tebbe, S., Leifker, K., Tholema, N., Quick, M. and Schmid, R. (1998). Topology of the Na^+/proline transporter of *Escherichia coli*. J. Biol. Chem. *273*, 26400–26407.

Jung, K., Voss, J., He, M., Hubbell, W. L. and Kaback, H. R. (1995). Engineering a metal binding site within a polytopic membrane protein, the lactose permease of *Escherichia coli*. Biochemistry *34*, 6272–6277.

Kensch, O., Connolly, B. A., Steinhoff, H. J., McGregor, A., Goody, R. S. and Restle, T. (2000a). HIV-1 reverse transcriptase-pseudoknot RNA aptamer interaction has a binding affinity in the low picomolar range coupled with high specificity. J. Biol. Chem. *275*, 18271–18278.

Kensch, O., Restle, T., Wöhrl, B. M., Goody, R. S. and Steinhoff, H.-J. (2000b). Temperature-dependent equilibrium between the open and close conformation of the p66 subunit of HIV-1 reverse transcriptase revealed by site-directed spin labelling. J. Mol. Biol. *301*, 1029–1039.

Kisker, C., Hinrichs, W., Tovar, K., Hillen, W. and Saenger, W. (1995). The complex formed between Tet repressor and tetracycline-Mg^{2+} reveals mechanism of antibiotic resistance. J. Mol. Biol. *247*, 260–280.

Klare, J., Bordignon, E., Engelhard, M. and Steinhoff, H.-J. (2004a). Sensory rhodopsin II and bacteriorhodopsin: light activated helix F movement. Photochem. Photobiol. Sci. *3*, 543–547.

Klare, J., Gordeliy,V. I., Labahn, J., Büldt, G., Steinhoff, H.-J. and Engelhard, M. (2004b). The archaeal sensory rhodopsin II/transducer complex: a model for transmembrane signal transfer. FEBS Lett. *564*, 219–224.

Koteiche, H. A. and Mchaourab, H. S. (1999). Folding pattern of the α-crystallin domain in αA-crystallin determined by site-directed spin labeling. J. Mol. Biol. *294*, 561–577.

Kurshev, V. V., Raitsimring, A. M. and Tsvetkov, Y. D. (1989). Selection of dipolar interaction by the 2+1 pulse train ESE. J. Magn. Reson. *81*, 441–454.

Leigh, J. S. (1970). ESR rigid lattice line shape in a system of two interacting spins. J. Chem. Phys. *52*, 2608–2612.

Luecke, H., Schobert, B., Richter, H. T., Cartailler, J. P. and Lanyi, J. K. (1999). Structure of bacteriorhodopsin at 1.55 Å resolution. J. Mol. Biol. *291*, 899–911.

Mchaourab, H. S. and Perozo, E. (2000). Determination of protein folds and conformational dynamics using spin-labeling EPR spectroscopy. In: Distance Measurements in Biological Systems by EPR, L. J. Berliner, S.S. Eaton and G.R. Eaton, eds. (New York, USA: Kluwer).

Müller, G., Hecht, B., Helbl, V., Hinrichs, W., Saenger, W. and Hillen, W. (1995). Characterization of non-inducible Tet repressor mutants suggests conformational changes necessary for induction. Nat. Struct. Biol. *2*, 693–703.

Orth, P., Schnappinger, D., Hillen, W., Saenger, W. and Hinrichs, W. (2000). Structural basis of gene regulation by the tetracycline inducible Tet repressor-operator system. Nat. Struct. Biol. *7*, 215–219.

Pannier, M., Veit, S., Godt, A., Jeschke, G. and Spiess, H. W. (2000). Dead-time free measurement of dipole-dipole interactions between electron spins. J. Magn. Reson. *142*, 331–340.

Perozo, E. and Rees, D. C. (2003). Structure and mechanism in prokaryotic mechanosensitive channels. Curr. Opin. Struct. Biol. *13*, 432–442.

Perozo, E., Cortes, D. M. and Cuello, L. G. (1998). Three-dimensional architecture of a K^+ channel: implications for the mechanism of ion channel gating. Nat. Struct. Biol. *5*, 459–469.

Perozo, E., Cortes, D. M. and Cuello, L. G. (1999). Structural rearrangement underlying K^+-channel activation gating. Science *285*, 73–78.

Perozo, E., Cortes, D. M., Sompornpisut, P., Kloda, A. and Martinac, B. (2002). Open channel structure of MscL and the gating mechanism of mechanosensitive channels. Nature *418*, 942–948.

Persson, M., Harbridge, J. R., Hammarstrom, P., Mitri, R., Martensson, L. G., Carlsson, U., Eaton, G. R. and Eaton, S. S. (2001). Comparison of electron paramagnetic resonance methods to determine distances between spin labels on human carbonic anhydrase II. Biophys. J. *80*, 2886–2897.

Quick, M. and Jung, H. (1998). A conserved aspartate residue, Asp187, is important for Na^+-dependent proline binding and transport by the Na^+/proline transporter of *Escherichia coli*. Biochemistry *37*, 13800–13806.

Quick, M., Stölting, S. and Jung, H. (1999). Role of conserved Arg40 and Arg117 in the Na^+/proline transporter of *Escherichia coli*. Biochemistry *38*, 13523–13529.

Rabenstein, M. D. and Shin, Y. K. (1995). Determination of the distance between two spin labels attached to a macromolecule. Proc. Natl. Acad. Sci. USA *92*, 8239–8243.

Radzwill, N. (2001). Bestimmung der Strukturänderungen der lichtgetriebenen Protonenpumpe Bakteriorhodopsin mittels zweifacher Spinmarkierung und ESR-Spektroskopie. PhD Thesis, University of Bochum, Germany.

Radzwill, N., Gerwert, K. and Steinhoff, H.-J. (2001). Time-resolved detection of transient movement of helices F and G in doubly spin-labeled bacteriorhodopsin. Biophys. J. *80*, 2856–2866.

Schiemann, O., Piton, N., Mu, Y., Stock, G., Engels, J. W. and Prisner, T. F. (2004). A PELDOR-based nanometer distance ruler for oligonucleotides. J. Am. Chem. Soc. *126*, 5722–5729.

Skalka, A. and Goff, S. (1993). Reverse Transcriptase (Cold Spring Habor, USA: Cold Spring Habor Laboratory Press).

Spudich, J. L. (1998). Variations on a molecular switch – transport and sensory signalling by archaeal rhodopsins. Mol. Microbiol. *28*, 1051–1058.

Spudich, J. L., Yang, C. S., Jung, K. H. and Spudich, E. N. (2000). Retinylidene proteins: structures and functions from archaea to humans. Annu. Rev. Cell Dev. Biol. *16*, 365–392.

Steinhoff, H.-J. (2002). Methods for study of protein dynamics and protein-protein interaction in protein-ubiquitination by electron paramagnetic resonance spectroscopy. Frontiers Biosci. *7*, c97–110.

Steinhoff, H.-J. and Suess, B. (2003). Molecular mechanism of gene regulation by site-directed spin labeling. Methods *29*, 188–195.

Steinhoff, H.-J., Dombrowsky, O., Karim, C. and Schneiderhahn, C. (1991). Two dimensional diffusion of small molecules on protein surfaces: an EPR study of the restricted translational diffusion of protein-bound spin labels. Eur. Biophys. J. *20*, 293–303.

Steinhoff, H. J., Mollaaghababa, R., Altenbach, C., Hideg, K., Krebs, M., Khorana, H. G. and Hubbell, W. L. (1994). Time-resolved detection of structural changes during the photocycle of spin-labeled bacteriorhodopsin. Science *266*, 105–107.

Steinhoff, H. J., Radzwill, N., Thevis, W., Lenz, V., Brandenburg, D., Antson, A., Dodson, G. and Wollmer, A. (1997). Determination of interspin distances between spin labels attached to insulin: comparison of electron paramagnetic resonance data with the X-ray structure. Biophys. J. *73*, 3287–3298.

Steinhoff, H. J., Müller, M., Beier, C. and Pfeiffer, M. (2000a). Molecular dynamics simulation and EPR spectroscopy of nitroxide side chains in bacteriorhodopsin. J. Mol. Liquids *84*, 17–27.

Steinhoff, H.-J., Savitsky, A., Wegener, C., Pfeiffer, M., Plato, M. and Möbius, K. (2000b). High-field EPR studies of the structure and conformational changes of site-directed spin labeled bacteriorhodopsin. Biochim. Biophys. Acta *1457*, 253–262.

Thorgeirsson, T. E., Xiao, W. Z., Brown, L. S., Needleman, R., Lanyi, J. K. and Shin, Y. K. (1997). Transient channel-opening in bacteriorhodopsin – an EPR study. J. Mol. Biol. *273*, 951–957.

Tiebel, B., Radzwill, N., Aung-Hilbrich, L. M., Helbl, V., Steinhoff, H. J. and Hillen, W. (1999). Domain motions accompanying Tet repressor induction defined by changes of interspin distances at selectively labeled sites. J. Mol. Biol. *290*, 229–240.

Voss, J., Hubbell, W. L. and Kaback, H. R. (1995a). Distance determination in proteins using designed metal ion binding sites and site-directed spin labeling – application to the lactose permease of *Escherichia coli*. Proc. Natl. Acad. Sci. USA *92*, 12300–12303.

Voss, J., Salwinski, L., Kaback, H. R. and Hubbell, W. L. (1995b). A method for distance determination in proteins using a designed metal ion binding site and site-directed spin labeling – evaluation with T4 lysozyme. Proc. Natl. Acad. Sci. USA *92*, 12295–12299.

Voss, J., Hubbell, W. L. and Kaback, H. R. (1998). Helix packing in the lactose permease determined by metal-nitroxide interaction. Biochemistry *37*, 211–216.

Wegener, A. A., Chizhov, I., Engelhard, M. and Steinhoff, H.-J. (2000a). Time-resolved detection of transient movement of helix F in spin-labelled pharaonis sensory rhodopsin II. J. Mol. Biol. *301*, 881–891.

Wegener, C., Tebbe, S., Steinhoff, H.-J. and Jung, H. R. (2000b). Spin labeling analysis of structure and dynamics of the Na^+/proline transporter of *Escherichia coli*. Biochemistry *39*, 4831–4837.

Wegener, A. A., Klare, J. P., Engelhard, M. and Steinhoff, H.-J. (2001a). Structural insights into the early steps of receptor-transducer signal transfer in archaeal phototaxis. EMBO J. *20*, 5312–5319.

Wegener, C., Savitsky, A., Pfeiffer, M., Möbius, K. and Steinhoff, H.-J. (2001b). High-field EPR-detected shifts of magnetic tensor components of spin label side chains reveal protein conformational changes: the proton entrance channel of bacteriorhodopsin. Appl. Magnet. Res. *21*, 441–452.

Xiao, W., Brown, L. S., Needleman, R., Lanyi, J. K. and Shin, Y.-K. (2000). Light-induced rotation of a transmembrane a-helix in bacteriorhodopsin. J. Mol. Biol. *304*, 715–721.

Yan, B., Takahashi, T., Johnson, R. and Spudich, J. L. (1991). Identification of signaling states of a sensory receptor by modulation of lifetimes of stimulus-induced conformations: the case of sensory rhodopsin II. Biochemistry *30*, 10686–10692.